

Observation of Kilohertz Quasiperiodic Oscillations from the Atoll Source 4U 1702–429 by *RXTE*

Craig B. Markwardt^{1,2}, Tod E. Strohmayer¹, Jean H. Swank¹

ABSTRACT

We present results of *Rossi X-Ray Timing Explorer* (*RXTE*) observations of the atoll source 4U 1702–429 in the middle of its luminosity range. Kilohertz-range quasiperiodic oscillations (QPOs) were observed first as a narrow (FWHM ~ 7 Hz) peak near 900 Hz, and later as a pair consisting of a narrow peak in the range 625–825 Hz and a faint broad (FWHM 91 Hz) peak. When the two peaks appeared simultaneously the separation was 333 ± 5 Hz. Six type I thermonuclear bursts were detected, of which five exhibited almost coherent oscillations near 330 Hz, which makes 4U 1702–429 only the second source to show burst oscillations very close to the kilohertz QPO separation frequency. The energy spectrum and color-color diagram indicate that the source executed variations in the range between the “island” and “lower banana” atoll states. In addition to the kilohertz variability, oscillations at ~ 10 , ~ 35 , and 80 Hz were also detected at various times, superimposed on a red noise continuum. The centroid of the ~ 35 Hz QPO tracks the frequency of the kilohertz oscillation when they were both present. A Lense-Thirring gravitomagnetic precession interpretation appears more plausible in this case, compared to other atoll sources with low frequency QPOs.

Subject headings: accretion, accretion disks — stars: individual (4U 1702–429)
— stars: neutron

1. Introduction

Since the discovery of kilohertz (400–1200 Hz) quasiperiodic oscillations (QPOs) from 4U 1728–34 (Strohmayer et al 1996) and Sco X-1 (van der Klis et al 1996) with the

¹NASA/Goddard Space Flight Center, Code 662, Greenbelt, MD 20771; craigm@lheamail.gsfc.nasa.gov (CBM); stroh@lheamail.gsfc.nasa.gov (TES); swank@pcasun1.gsfc.nasa.gov (JHS)

²National Research Council Resident Associate

Rossi X-Ray Timing Explorer (RXTE), there has been a concerted effort to characterize the phenomenon by examining a variety of low mass X-ray binary systems. To date nearly twenty such sources have been discovered (van der Klis 1998; Strohmayer, Swank, & Zhang 1998), and a general pattern has emerged. In nearly all of the sources two kilohertz QPO peaks are seen. Both QPO frequencies increase and decrease as the source intensity and spectrum changes, but the separation between the two remains very nearly constant, suggesting a beat interpretation (Strohmayer et al 1996; Miller, Lamb & Psaltis 1998), although this is not always so in observation or theory (van der Klis et al 1996; Titarchuk, Lapidus & Muslimov 1998). A third, nearly coherent oscillation is also seen sometimes during type I thermonuclear bursts, near frequencies either one or two times the separation frequency between the two kilohertz peaks, and suggests that the neutron star spin frequency is observed directly.

In this Letter we present our findings from *RXTE* observations of the atoll source 4U 1702–429 (Oosterbroek et al 1991), on 1997 July 19–30 when it exhibited both two kilohertz QPO peaks and bursts with oscillations. Preliminary results from a part of the data have already been presented by Strohmayer, Swank & Zhang (1998). Strong kilohertz oscillations from 625–925 Hz were easily detected in several portions of the persistent emission of the source. A second, much broader kilohertz peak was also detected at higher frequencies using a sensitivity-enhancing averaging technique advanced by Méndez et al (1998a). We also detected QPO and noise features in the 1–100 Hz frequency range, which changed during the observation. Six type I bursts were seen, of which five exhibited sharp QPOs near 330 Hz.

2. Observations

Pointed observations of 4U 1702–429 by *RXTE* Proportional Counter Array (PCA) occurred between 1997 July 19, 21, 26, and 30, for a total exposure of approximately 101 ks. In addition to the “Standard” modes, data were also collected in an “event” mode with 125 microsecond timing and spectral information for individual X-ray events. Burst “trigger” and “catcher” modes were also used. The average source intensity changed significantly over the course of the observation; average background subtracted rates (2.5–16 keV) were 670 s^{-1} July 19 and July 21, 990 s^{-1} July 26, and 859 s^{-1} July 30. We used the background models based on the “Very Large Event” (VLE) rate and the activation rate during non-source sky observations (model version 1). The color-color diagram is shown in Figure 1.

The color differences reflect spectral differences which are significant, although not

large. For the persistent flux, the Standard 2 spectral data were gathered for intervals with similar temporal behavior, using only data up to 30 keV in the top layer of detector anodes of all proportional counters. A systematic error of 1.5% was added (this error was needed to fit contemporaneous Crab data). Acceptable fits were obtained with a cut off power law spectrum $E^{-\gamma} \times \exp(-E/kT)$. For July 26 (10.3–13.8 UT) the photon index $\gamma = 0.35 \pm 0.03$ and $kT = 3.53 \pm 0.04$ keV, while for July 30 (8.5–12.0 UT) $\gamma = 0.80 \pm 0.03$, and $kT = 4.56 \pm 0.07$. Plausibly, the steeper power law and higher kT correspond to upper left points in Figure 1, the flatter power law and lower kT to the rightmost points in the figure. The flux ranged from $1.7(1.3) \times 10^{-9}$ erg cm $^{-2}$ s $^{-1}$ on July 19 and 21 to $2.6(2.0) \times 10^{-9}$ erg cm $^{-2}$ s $^{-1}$ on July 26, for 1.6–30 (2–10) keV. These values overlap those reported for previous observations (Christian & Swank 1997; Oosterbroek et al 1991).

3. Kilohertz Variability

Event data for channels 0–79 (0.03–29.1 keV) were used to construct power spectra in 8 s segments, which were then averaged in groups of 16 (i.e., averaged over 128 s) to increase signal to noise. Power spectra on July 19 have a faint but significant QPO feature near 890–910 Hz with a full width at half maximum (FWHM) of 32 Hz and RMS amplitude of 6.2%. The frequency changes significantly during the observation. A narrow but lower frequency QPO appears in the July 30 observations, during which the frequency of the QPO wanders continuously between 625–825 Hz, with a mean frequency of 722 Hz. The presence and absence of these high frequency QPOs is indicated in Figure 1.

A heavily rebinned spectrum of July 30 indicated a much fainter and broader peak at about 1000 Hz was present, which tracked the lower peak. To more precisely determine the parameters of the upper and lower peak, the “shift and average” technique was employed to align the lower peak. This technique was first applied to find a weaker upper QPO peak in 4U 1608–52 (Méndez et al 1998a), and is optimal when the peak separation remains constant or nearly so. The centroid of the lower strong and narrow peak was fitted in each 128 s spectrum individually. The spectra were then shifted so that the centroid frequency became the mean fitted frequency (722 Hz). Finally the spectra were averaged, producing a strong single peak at 722 Hz. (Figure 2). The same technique was applied to data from July 19, except that all peaks were aligned to the average frequency of 902 Hz.

The power spectrum of July 30 clearly shows a second broader peak at approximately 1050 Hz (the average centroid frequency of the upper peak). We fitted the average July 30 spectrum with a model composed of a constant (representing Poisson noise level) and two Lorentzian peaks, where the upper peak centroid frequency was parameterized in terms of

an offset $\Delta\nu$ from the lower peak. The best-fit parameters of the model are in Table 1, and show the upper peak was detected at a very high significance on July 30 at a separation of 333 ± 5 Hz from the lower peak. On July 19 when the narrow QPO was present at ~ 900 Hz there was no evidence for a second peak; the 95% confidence limits for the RMS amplitude of QPOs having a FWHM 10 and 100 Hz are 1.7% and 2.9%, respectively. No QPO peaks were present on July 21 or July 26 individually. Combined, the 95% confidence upper limits for both days are 1.2% and 2.0% for QPOs with FWHMs of 10 and 100 Hz, respectively.

Both QPOs are similar to those observed from other kilohertz QPO sources. In cases where the high frequency QPOs were detected, the fractional RMS amplitude increases with energy. On July 30, the RMS fraction of the lower peak increased monotonically from 5.5% to 10.7% to 13.1% in the channel ranges 0 to 17 (0.03–6.2 keV), 18 to 26 (6.5–9.4 keV) and 27 to 79 (9.8–29.1 keV); the amplitude was about 30% less on July 19. The amplitude of the upper peak on July 30, the only day it was detected, increased from 3.5% to 6.1% to 12.5% in the same energy bands.

In both Sco X-1 and 4U 1608–52, the separation between upper and lower QPO frequencies is not a constant, but rather decreases with either count rate or the lower QPO frequency (van der Klis et al 1997; Méndez et al 1998b). On July 30, when the upper peak is detected, the centroid frequency of the lower peak varies from 625–825 Hz. We attempted to determine whether the frequency separation also varies by grouping the individual 128 s power spectra in ranges according to the lower QPO centroid frequency before shifting: <675 Hz, $675\text{--}725$ Hz, and >725 Hz. Above 725 Hz the upper peak becomes weaker, and degraded statistics prevent further divisions. The groups were shifted and averaged, and fitted by the same model as in Table 1. The inset of Figure 2 shows the fitted frequency separation as a function of the lower QPO frequency. The three spectra were also fitted to a model where the separation was held fixed. An F -test indicates that the hypothesis of constant separation can be rejected at only a 1.5σ confidence level. Nevertheless, the general trend in Figure 2 is similar to that seen in both 4U 1608–52 and Sco X-1.

4. Lower Frequency Variability

4U 1702–429 also exhibits transient variability at frequencies below 100 Hz; at several points during the observation both QPO and broad band noise features were observed. Figure 3 shows a representative sample of average unshifted³ 64 s power spectra. Between

³The linear shifting process used to align the 625–825 Hz and 900 Hz QPOs corrupts the power spectrum at lower frequencies.

July 26.6–26.9, when no kilohertz QPOs were present, the source had a very strong 80 Hz QPO and a lower frequency band limited complex of variability between 5–60 Hz. We fitted the power spectrum with a model consisting of a constant, a power law, and up to three Lorentzian functions. The best fit QPO parameters for the observations are given in Table 1, and the representative models are plotted in Figure 3. When the two kilohertz QPOs returned on July 30, only a single 35 Hz QPO peak was seen (Figure 3, upper curve). On both days, the continuum extended to about 1 mHz, where a turnover was evident. The noise continuum changed over the observation, with power law indices of -0.79 ± 0.06 , -1.68 ± 0.09 , -1.63 ± 0.08 , and -0.517 ± 0.035 on July 19, 21, 26, 30, respectively. The integrated low frequency noise ($5 \times 10^{-4} - 3 \times 10^{-2}$ Hz) was 1.8, 3.4, 4.0 and 1.7% for the same days.

Although there does not appear to be a direct harmonic relationship between any of the QPO frequencies below 100 Hz, the centroid of the 35 Hz peak on July 30 is correlated with the centroid of the simultaneously-present kilohertz QPOs. We found that as the mean kilohertz QPO frequency increased in each band from 657 Hz to 702 Hz to 769 Hz, the low frequency QPO centroid increased from 32.9 ± 0.6 Hz to 34.8 ± 0.6 Hz to 40.1 ± 0.8 Hz, thus establishing a ratio of ~ 19.5 between the two. This linkage between the kilohertz and lower frequency QPOs is similar to that seen previously (e.g. Sco X-1, van der Klis et al 1996; 4U 1728–34, Ford & van der Klis 1998).

5. Burst Oscillations

A total of six type I (thermonuclear) X-ray bursts occurred during the observations. The peak PCA count rate (2–90 keV) during the bursts ranged from a low of 14,000 ct s⁻¹ to a maximum of 26,000 ct s⁻¹. To search for pulsations we used the 2–90 keV burst mode high time resolution data to compute power spectra from consecutive 2 s intervals beginning near the peak of each burst. We detected pulsations at ≈ 330 Hz in five of the six bursts. Pulsation amplitudes in the 2–24 keV band ranged from a few percent to as high as 18% (RMS). The pulsation frequency increases during all the bursts, eventually reaching an upper, limiting frequency in the decaying tail of the burst. This behavior is nearly identical to the frequency evolution of pulsations observed in bursts from 4U 1728–34 and other sources with oscillations during bursts (see Strohmayer et al. 1998; and Strohmayer, Swank & Zhang 1998). To illustrate this behavior we computed dynamic power spectra for each burst using 2 s intervals with a new interval beginning every 0.125 s. Figure 4 shows such a dynamic power spectrum computed for the burst observed on 1997 July 26 at 14:04:19 UT, with the PCA countrate overlaid. The run of frequency during this burst of relatively low

peak luminosity was similar to that of the high luminosity burst shown in Strohmayer, Swank, & Zhang (1998). We will present a more comprehensive timing and spectral analysis of the bursts in a subsequent publication.

6. Discussion and Conclusions

Atoll burst sources range in estimated luminosity from a hundredth to perhaps a third of the Eddington limit for neutron stars. Kilohertz-range QPOs have been seen in sources throughout this luminosity range. 4U 1702–429 is an atoll burst source with a luminosity, assuming a distance of 7 kpc (Oosterbroek et al 1991), of about 1×10^{37} erg s^{−1} which is similar to that of 4U 1728–34 and 4U 1705–44. We found that 4U 1702–429, like 4U 1728–34 (Strohmayer et al. 1996) also exhibits two kilohertz QPOs with a separation of about 330 Hz, to be compared to 363 Hz for 4U 1728–34. Furthermore, five bursts exhibited flux oscillations within a few Hertz of 330 Hz. This makes 4U 1702–429 only the second source in which the dominant burst power is at the frequency of the difference between the two higher frequencies seen in the persistent flux. The lower QPO peak has been interpreted as a beat between the upper peak and the neutron star spin frequency (Miller, Lamb & Psaltis 1998). The separation between the two kilohertz peaks is approximately constant for several sources, and is thought to be the neutron star spin frequency. Our results here are consistent with a constant separation, although a small variation is suggested.

On July 30, when both peaks are observed, the highest frequency of the upper QPO is inferred to be at least 1156 Hz, assuming the peak separation is 333 Hz. Given that the lower peak on July 30 is quite narrow compared to the upper one, it seems likely that the single peak that appears on July 19 is also a “lower” peak based on its width. If that is so, then we might speculate that the maximum upper frequency, although not detected, is as high as ~ 1230 Hz. In either case, the range of 1100–1200 Hz is consistent with the maximum frequency observed in other kilohertz QPO sources. The small changes in burst frequency during the burst are similar to those of 4U 1728–34 (Strohmayer et al. 1996) and the oscillations appear equally as consistent with rotation of a single spot on the neutron star.

The *RXTE* All-Sky Monitor record of 4U 1702–429 shows that the source intensity range is about 25–100 mCrab. During the week spanning the observations, the range was about 70–90 mCrab, yet the source exhibited markedly varied behavior. The atoll sources were defined by Hasinger and van der Klis (1989) in terms of both crude spectral behavior (color-color diagrams) and the continuum shape of the power spectra, based on *EXOSAT* data. The hard and soft colors trace a curve reminiscent of an atoll, comprised of an

“island” and a crescent shaped “banana” branch. In the power spectra low frequency noise is prevalent on the banana branches, and flat high frequency noise identifies the island state. In *RXTE* data a pattern has emerged in which the kilohertz QPO appear to be present in the lower banana and at least part of the island state (e.g., 4U 1608–52, Méndez et al 1998a; Aql X-1, Cui et al 1998; 4U 1735–44, Wijnands et al 1998; 4U 1820–30, Zhang et al. 1998). Even with the limited excursions of our observations, the color-color diagram suggests that 4U 1702–429 behaves similarly. If we follow the behavior of the other sources, then we would predict that the kilohertz QPOs would fade out during the flares and possibly at minimum flux.

These observations may not have quite reached the island state, which is described as having band limited white noise with a cut-off near the low-frequency QPO. The continuum portion of the power spectrum of July 30, while shallower than July 26, was not flat. On the other hand, the power spectrum of July 26 which has a steep low frequency component, and is thus presumably in an intermediate banana state, also has unaccounted-for QPO-like structures. We should note that the color-color diagram suggests the banana branch may not be unique.

A strong 35 Hz feature accompanies the kilohertz QPOs, and while the lower kilohertz QPO does not have large excursions, the two do appear to track each other. This behavior might be expected if the 35 Hz QPO represented Lense-Thirring precession of a warped inner accretion disk under the influence of a spinning compact body (Stella & Vietri 1998). The theory predicts oscillations in the tens of hertz range, depending on the ratio of the moment of inertia ($I = I_{45}10^{45}$ g cm²) to the mass of the neutron star M . Assuming the neutron star spin frequency is 330 Hz, the Kepler frequency at the inner edge of the accretion disk is 330 Hz higher than the lower peak, and the ratio $I_{45}M_{\odot}/M$ is a free parameter, we fit to the functional form of Stella & Vietri (1998), and find a ratio of 2.3 ± 0.1 . Although this value is too high for most neutron star equations of state, which approach unity (Marković & Lamb 1998), it is closer than the reported ratios of 4–5 for most other QPO sources with such measurements (e.g., 4U 1735–44, Wijnands et al 1998; 4U 1728–34, Ford & van der Klis 1998).

The catalog of low frequency QPOs is indeed complex. A 35–40 Hz QPO accompanies the kilohertz QPOs but with varying width. The power spectrum of July 26 also shows a ~ 30 Hz QPO, as well as ~ 10 Hz and 80 Hz components, while on July 21 a peak at ~ 30 Hz is not present. Such QPOs have been detected in other atoll sources and may be comparable to the horizontal branch oscillations (HBO) of Z sources. However, the 80 Hz frequency observed here is one of the highest so far seen below 100 Hz in a neutron star system. The power spectrum of GX 13+1, an atoll source several times brighter than 4U 1702–429,

has interesting similarities to the power spectra we have seen for 4U 1702–429 when the kilohertz QPO were not seen. Homan et al. 1998 found a 57–61 Hz QPO when the source was in an upper part of a banana branch in the color-color diagram, along with very low frequency noise described by a power law of index -1.3 , and a peaked noise component. The power spectrum of 4U 1702–429 in the highest part of its banana branch contains similar components. Homan et al suggest the peaked noise and the QPO in GX 13+1 correspond to the low frequency noise (LFN) and HBO in Z sources and to the high frequency noise and low frequency QPO in atoll sources. It is interesting that 4U 1702–429 exhibits the atoll low frequency QPO (although not the noise) when the kilohertz QPO is present, and is similar to GX 13+1 when it is not present.

REFERENCES

- Christian, D. J., & Swank, J. H. 1997, *ApJS*, 109, 177
- Cui, W., Barret, D., Zhang, S. N., Chen, W., Boirin, L., & Swank, J. 1998, *ApJ*, 502, L49
- Ford, E. C., & van der Klis, M. 1998, *ApJ*, 506, L39
- Hasinger, G., & van der Klis, M. 1989, *A&A*, 225, 79
- Homan, J., van der Klis, M., Wijnands, R., Vaughan, B., & Kuulkers, E. 1998, *ApJ*, 499, L41
- Méndez, M., van der Klis, M., van Paradijs, J., Lewin, W. H. G., Vaughan, B. A., Kuulkers, E., Zhang, W., Lamb, F. K., & Psaltis, D. 1998a, *ApJ*, 494, L65
- Méndez, M., van der Klis, M., Wijnands, R., Ford, E., van Paradijs, J., & Vaughan, B. A. 1998, *ApJ*, 505, L23
- Marković, D., & Lamb, F. K. 1998, *ApJ*, 507, 316
- Miller, M. C., Lamb, F. K., & Psaltis, D. 1998, *ApJS*, in press
- Oosterbroek, T., Phenninx, W. van der Klis, M., van Paradijs, & J., Lewin, W. H. G. 1991, *A&A*, 250, 389
- Stella, L., & Vietri, M. 1998, *ApJ*, 492, L59
- Strohmayer, T. E., Swank, J. H., & Zhang, W. 1998, *Nuclear Physics B (Proc. Suppl.)* 69/1-3, 129
- Strohmayer, T. E., Zhang, W., Swank, J. H., & Lapidus, I., 1998, *ApJ*, 503, L147
- Strohmayer, T. E., Zhang, W., Swank, J. H., Smale, A., Titarchuk, L., Day, C., & Lee, U. 1996, *ApJ*, 469, L9
- Titarchuk, L., Lapidus, I., Muslimov, A. 1998, *ApJ*, 499, 315
- van der Klis, M. 1998, *Nuclear Physics B (Proc. Suppl)* 69/1-3, 103
- van der Klis, M., Swank, J. H., Zhang, W., Jahoda, K., Morgan, E. H., Lewin, W. H. G., Vaughan, B., & van Paradijs, J. 1996, *ApJ*, 469, L1
- van der Klis, M., Wijnands, R. A. D., Horne, K., & Chen, W. 1997, *ApJ*, 481, L97
- Wijnands, R., van der Klis, M., Méndez, M., van Paradijs, J., Lewin, W. H. G., Lamb, F. K., Vaughan, B., & Kuulkers, E. 1998, *ApJ*, 495, L39
- Wijnands, R., & van der Klis, M. 1998, *ApJ*, in press (astro-ph/9810342)
- Zhang, W., Smale, A. P., Strohmayer, T. E., & Swank, J. H. 1998, *ApJ*, 500, L171

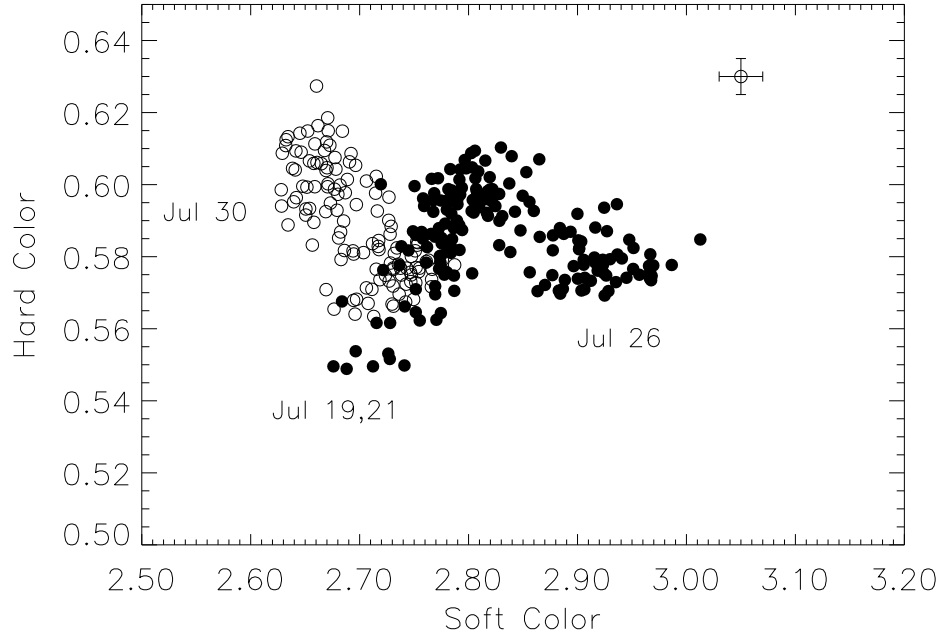


Fig. 1.— X-ray color-color diagram of 4U 1702-429. Each point represents a 256 s average over the 16 s ratios, excluding bursts, when all 5 detectors were on. Intervals in which kilohertz QPO were observed are represented by open circles. The filled circles represent intervals in which no kilohertz QPO is detected. The “Hard color” is the ratio of counts in the 9.43–16.0 keV and 6.52–9.43 keV bands and the “Soft color” is the ratio in the 3.63–6.52 keV and 1.86–3.63 keV bands.

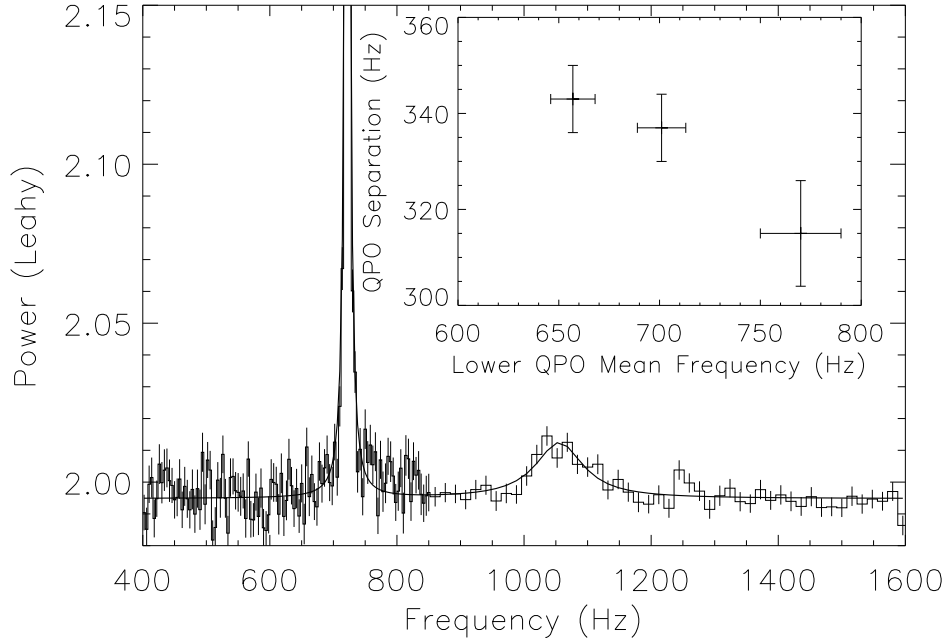


Fig. 2.— Average 2–25 keV PCA power spectrum for observations on July 30, after shifting the centroid of the lower peak to 722 Hz. The lower half of the spectrum has 4 Hz frequency bins, while the upper half is rebinned to 16 Hz bins for display purposes to enhance the broad faint 1050 Hz peak. The inset shows the fitted QPO separation as a function of the mean lower QPO frequency (see text). Horizontal error bars represent the standard deviation of frequencies in the chosen band.

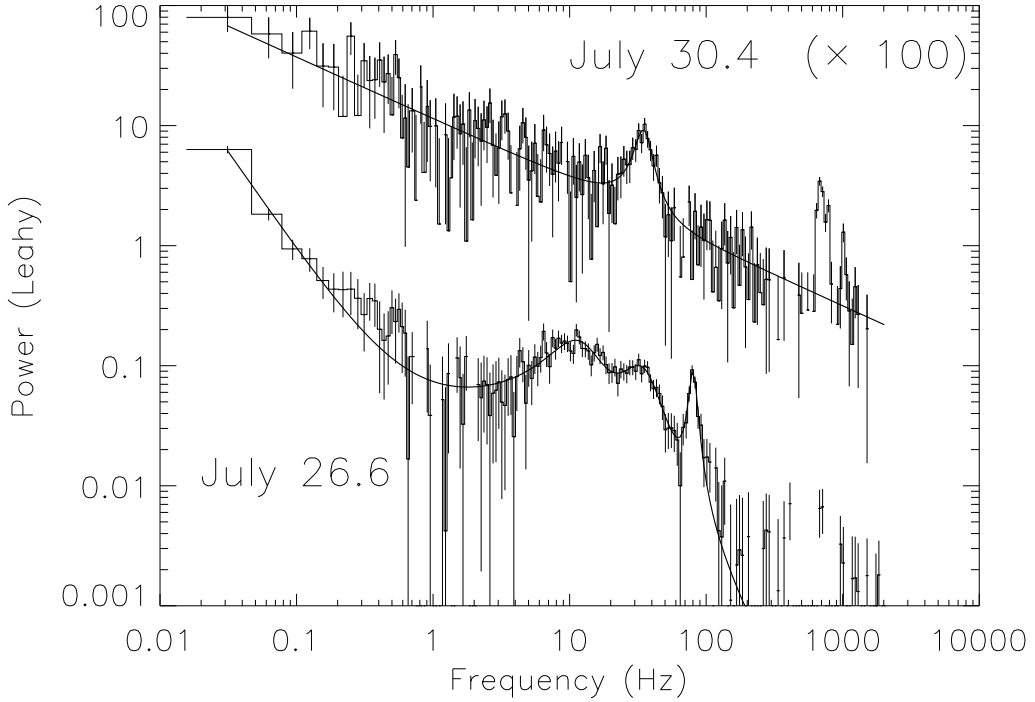


Fig. 3.— Broadband power spectrum of 4U 1702–429 starting on July 26.6 (bottom curve) and July 30.4 (top curve) in the channel range 18 to 79 (6–26.3 keV), after subtracting the Poisson noise level. The upper curve has been offset by two decades for clarity. The continuous curves indicate the best fitting power law plus Lorentzian model for each power spectrum. A ~ 800 Hz QPO peak, unaligned in this representation, appears on July 30 but did not enter into the fit.

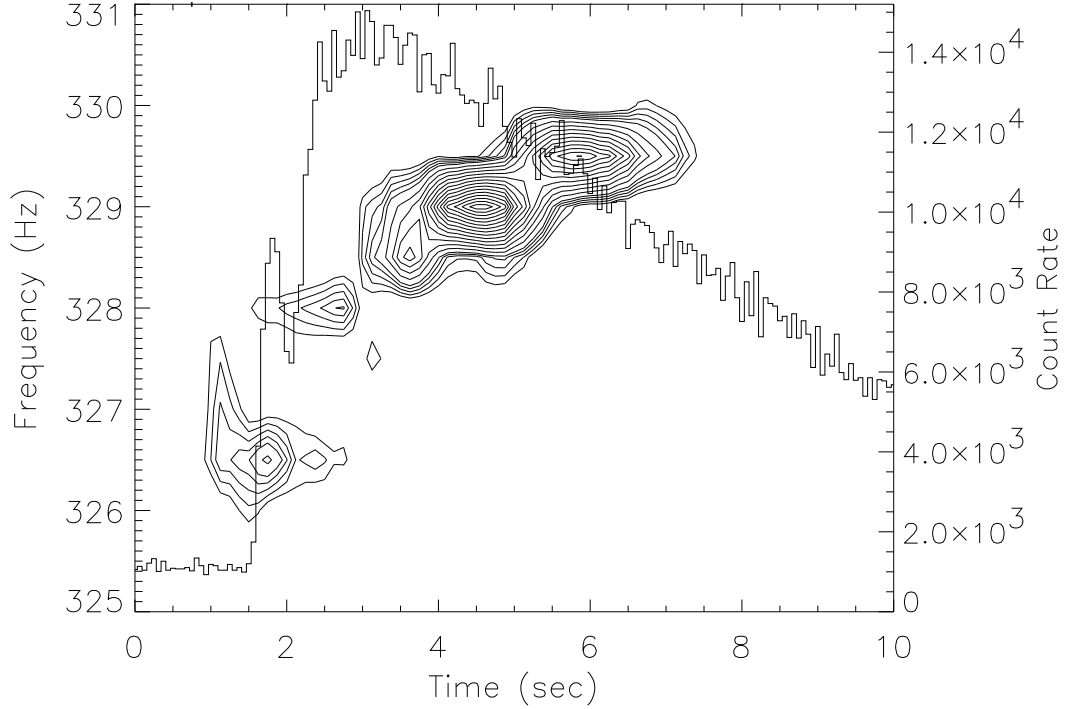


Fig. 4.— Dynamic power spectrum showing ≈ 330 Hz pulsations during a burst from 4U 1702–429. The contours denote loci of constant Fourier power as a function of frequency (left ordinate) and time. The individual power spectra were computed from 2 s intervals sampled at $1/8192$ s time resolution, with a new interval beginning every 0.125 s. The PCA countrate versus time is also shown (right ordinate). The power spectral contours were aligned on the center of each 2 s interval.

Table 1: Temporal Properties of 4U 1702–429

Date	Frequency (Hz)	RMS (%)	FWHM (Hz)
Jul 19.37–19.86	$\nu = 902^a$	6.0 ± 0.1	6.1 ± 0.3
	$\nu = 39.0 \pm 3.4$	5.3 ± 0.8	27 ± 10
Jul 21.01–21.17	$\nu = 85.6 \pm 3.7$	9.6 ± 0.8	51.5 ± 11.6
	$\nu = 12.0 \pm 1.0$	7.7 ± 0.6	15.7 ± 0.9
Jul 26.60–26.93	$\nu = 80.1 \pm 0.5$	6.0 ± 0.3	12.0 ± 1.7
	$\nu = 32.5 \pm 1.2$	9.1 ± 1.1	26.2 ± 3.6
	$\nu = 10.8 \pm 0.4$	7.9 ± 0.5	12.4 ± 1.6
Jul 30.46–30.72	$\nu = 722^a$	7.78 ± 0.08	7.22 ± 0.18
	$\Delta\nu = 333 \pm 5^b$	5.33 ± 0.40	91 ± 17
	$\nu = 34.7 \pm 0.6$	6.3 ± 0.4	12.6 ± 2.0

^athe mean fitted QPO frequency before shifting (see text).

^bthe frequency *difference* from the lower peak.